Physicochem. Probl. Miner. Process., 61(4), 2025, 207418

http://www.journalssystem.com/ppmp

Physicochemical Problems of Mineral Processing

ISSN 1643-1049

Flotation separation of pyrrhotite from magnetite using sodium fluosilicate (Na_2SiF_6) as a selective activator

Xiaohui Zeng [1], Xin Hu [2], Zishuai Liu [2], Gan Wan [3]

[1] Wanguo Gold Group Co., Ltd, Yichun 336305, China

[2] Jiangxi Provincial Key Laboratory of Low-Carbon Processing and Utilization of Strategic Metal Mineral Resources, Jiangxi University of Science and Technology, Ganzhou 341000, China

[3] Ganzhou Polytechnic, Ganzhou, 341008, China

Corresponding author: liuzishuai87@126.com (Zishuai Liu)

Abstract: Pyrrhotite and magnetite exhibit similar magnetic properties and oxidation susceptibility, posing significant challenges to their effective separation. This study investigated the flotation separation of pyrrhotite and magnetite using sodium fluorosilicate (SF) as an activator and xanthate as a collector. Single-mineral flotation tests demonstrated that SF effectively activated pyrrhotite flotation, enhancing its recovery rate. For artificially mixed ores with an initial sulfur grade of 19.79%, flotation achieved a concentrate with 39.32% sulfur content and 46.64% recovery, realizing efficient separation. Under the conditions of sulfur and iron grades of 2.60% and 61.34% respectively in the real ore feed, a sulfur concentrate with a yield of 25.80%, sulfur grade of 9.15%, and sulfur recovery rate of 90.86% was obtained, as well as an iron concentrate with a yield of 74.20%, iron grade of 63.08%, and iron recovery rate of 76.30%. This successfully achieved the objective of "increasing iron content and reducing sulfur content." Solution chemistry analysis, contact angle measurements, FTIR, and XPS investigations revealed the adsorption mechanisms of SF and xanthate on mineral surfaces. Results indicated that both SF and xanthate selectively adsorbed only on pyrrhotite surfaces. Furthermore, SF facilitated exposure of additional active sites on pyrrhotite, thereby promoting xanthate adsorption. These findings provide critical insights into the surface activation mechanism enabling effective pyrrhotite-magnetite separation.

Keywords: sodium fluorosilicate, selective activation mechanism, pyrrhotite, magnetite, flotation separation

1. Introduction

Iron ore resources in China are characterized by their "lean, fine, and complex" nature, posing significant challenges in exploitation. Despite abundant reserves, the prevalence of complex geological conditions and low-grade ores has led to a severe reliance on imported iron ore in China (over 80% sourced from Australia, Brazil, and India), resulting in significant supply chain vulnerabilities (Tang and Chen, 2022). In this context, the development of efficient mineral processing technology is urgently needed. Pyrrhotite ($Fe_{1-x}S$), as a key sulfide mineral coexisting with magnetite (Fe_3O_4), holds dual significance in terms of resource recovery and environmental sustainability (Yu et al., 2016; Liu et al., 2018). However, due to its similar specific magnetization coefficient and surface wettability to magnetite, conventional sorting processes suffer from serious cross contamination (Yuan et al., 2022). Currently, the lack of specialized flotation reagents and immature sorting processes have made desulfurization of iron concentrate a key bottleneck restricting industrial upgrading. Therefore, developing new magnetite sorting technology is not only the core path to achieve the quality goal of "increasing iron and reducing sulfur", but also a strategic choice to ensure resource security and promote green development.

Pyrrhotite, a common iron sulfide mineral frequently associated with complex sulfide deposits containing copper, nickel, and platinum-group metals, plays a pivotal role in determining resource utilization efficiency and metallurgical performance (Becker et al., 2010; Arvidson et al., 2013). Its flotation behavior demonstrates remarkable complexity due to its nonstoichiometric Fe/S ratio and

DOI: 10.37190/ppmp/207418

unique surface chemistry (Multani and Waters, 2018; Rezvani et al., 2024). For instance, surface oxidation generates hydrophilic iron oxides (e.g., FeOOH), significantly reducing natural floatability (Multani and Waters, 2018; Rezvani et al., 2024; Mikhlin et al., 2002). Current research focuses on surface modification and selective collector development. Although anionic collectors like butyl xanthate are widely used in sulfide mineral flotation, their adsorption efficiency on pyrrhotite is hindered by surface oxidation layers (Liao et al., 2023). Previous studies suggest that sulfuric acid enhances pyrrhotite flotation by dissolving hydrophilic iron oxide films and facilitating hydrophobic layer formation (Meng et al., 2023; Liu et al., 2018). Nevertheless, its strong acidity causes severe equipment corrosion, driving research toward metal ion activators. Copper sulfate has emerged as the predominant activator for sulfide mineral processing, owing to its unique utility in platinum-group metal beneficiation systems (Tang and Chen, 2022). The ongoing scientific debate concerning its activation mechanism primarily focuses on two principal mechanisms: ion exchange versus surface adsorption (Dai et al., 2022; Acar and Somasundaran, 1992). However, due to the tendency of copper ions (Cu^{2+}) to remain in tailings and wastewater, there is not only a risk of heavy metal pollution, but also the possibility of facing high environmental fines for exceeding environmental emission limits, which increases the compliance costs of enterprises. Sodium fluorosilicate (Na_2SiF_6, SF) also has activation potential in the flotation separation of pyrrhotite and magnetite. SF, as an environmentally friendly chemical product, has the characteristics of environmental performance, high added value, and sustainability. However, its mechanism of action in the flotation separation of pyrrhotite and magnetite is still lacking systematic understanding.

SF has emerged as a high-performance flotation reagent with multifunctional attributes, demonstrating exceptional efficacy in multicomponent ore separation processes. Its unique chemical architecture enables selective inhibition of silicate, carbonate, and associated gangue minerals via targeted adsorption and surface complexation mechanisms, thereby enhancing target mineral recovery rates. Recent systematic investigations into SF's interfacial interactions across diverse mineral systems have elucidated its pivotal role in resolving complex ore beneficiation challenges. In calcite-scheelite systems, SF achieves selective calcite depression through chemisorption of negatively charged species (F^-, $Si(OH)_2^{2-}$, SiF_6^{2-}, and $SiO(OH)_3^-$) onto surface Ca^{2+} sites, forming insoluble precipitates ($CaSiO_3$, CaF_2, and $CaSiF_6$) that suppress floatability, while scheelite remains unaffected (Dong et al., 2019). Analogously, in feldspar-quartz systems, SF-derived SiF_6^{2-} ions preferentially adsorb onto quartz surfaces, generating hydrophilic Si-O-F layers that sterically hinder collector adsorption, whereas feldspar retains inherent floatability, enabling efficient silicate separation (Hu et al., 2024). Notably, in rutile-hematite systems, SF coordinates with Fe^{3+} active sites on hematite surfaces via stable Fe-F bonding, effectively blocking collector attachment while preserving rutile floatability, thereby achieving enhanced flotation selectivity (Chen et al., 2020). Mechanistic studies reveal that SF's selective inhibition correlates directly with pH-dependent solution speciation (F^-, SiF_6^{2-}, $Si(OH)_3^-$) and mineral surface reactivity (e.g., metal coordination sites). Strategic modulation of operational parameters (pH, dosage) enables precise control over adsorption configurations, facilitating customized separation protocols for heterogeneous mineral assemblages. This molecular-level targeting mechanism not only advances critical metal recovery (e.g., Ti, W) from refractory ores but also pioneers sustainable pathways for eco-friendly reagent development and mineral interface chemistry research. Future research should further clarify the essential nature of its surface action, develop a synergistic system with new activators/collectors, and verify its industrial applicability through pilot-scale tests, so as to promote its wide application in the efficient utilization of refractory ore resources.

This study systematically investigates SF's activation mechanism in butyl xanthate-based pyrrhotite flotation through flotation tests, contact angle measurements, Fourier transform infrared spectroscopy (FTIR), and X-ray photoelectron spectroscopy (XPS). By elucidating SF's synergistic effects with xanthate collectors, we aim to establish theoretical foundations and technical frameworks for efficient pyrrhotite separation in complex sulfide ores.

2. Materials and methods

2.1. Materials

2.1.1. Minerals

The pyrrhotite ($Fe_{1-x}S_2$) and magnetite (Fe_3O_4) samples were sourced from Chifeng City, Inner Mongolia Autonomous Region, China. Pure mineral specimens were prepared through a standardized

comminution protocol involving sequential crushing, grinding, and wet-sieving processes to obtain target particle fractions.

Table 1. Chemical composition of pyrrhotite and magnetite (%)

Composition	Fe	S	Others
Pyrrhotite	56.52	38.55	4.93
Magnetite	68.21	0.04	31.75
Real ore	61.34	2.60	36.06

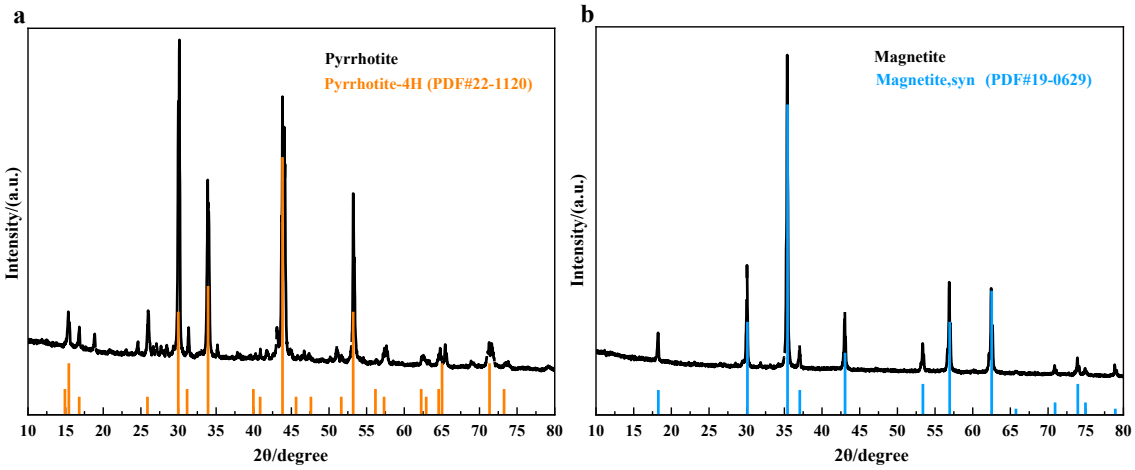

Fig. 1. XRD analysis of pyrrhotite (a) and maghemite (b)

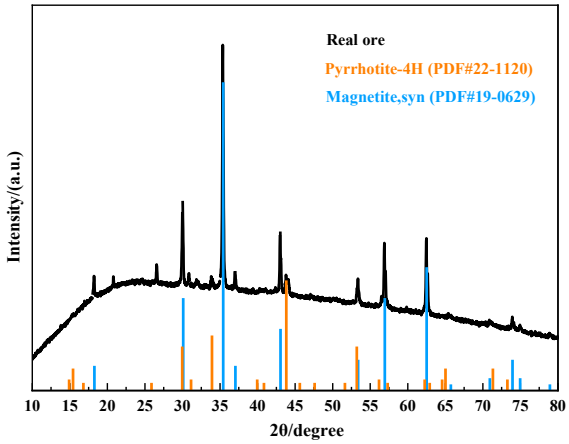

Fig. 2. XRD analysis of real ore

To explore the content of Fe and S in pure minerals of pyrrhotite, pure minerals of magnetite, and real ore, chemical multi-element analysis was conducted on these three minerals using titration method, and the results are shown in Table 1. The chemical multi-element analysis results in Table 1 preliminarily confirm the types of minerals. Among them, "others" in Table 1 mainly refers to other elements in minerals, mainly oxygen.

In addition, X-ray diffraction analysis was performed on pure pyrrhotite, pure minerals of magnetite, and real ore, and the relevant results are presented in Fig. 1 and Fig. 2 respectively.

As illustrated in Fig. 1, the XRD patterns of purified mineral specimens demonstrated exceptional phase congruence with reference PDF card data, satisfying stringent experimental requirements for subsequent flotation and surface characterization studies. The -0.074+0.038 mm fraction (200-400 mesh) was selectively allocated to batch flotation tests, while complementary particle size fractions were systematically employed for interfacial property investigations, including three-phase contact angle

measurements, Fourier-transform infrared spectroscopy (FTIR), and X-ray photoelectron spectroscopy (XPS) analyses.

The real ore was sourced from Wanguo Gold Group Co., Ltd., located in Jiangxi Province, China. Fig. 2 analysis revealed magnetite as the predominant valuable constituent in the real ore sample, with pyrrhotite occurring as the secondary mineralogical phase.

2.1.2. Chemical reagents

Deionized water was used throughout all experimental procedures. pH regulation was achieved using analytical-grade sulfuric acid (H_2SO_4, 95-98%) and sodium hydroxide (NaOH, ≥99%) solutions. The flotation system uses sodium hexafluorosilicate (Na_2SiF_6, 99.9%) as a surface activator and sodium butyl xanthate ($C_4H_9OCSSNa$, 97%) as a collector.

2.2. Flotation tests

2.2.1. Micro-flotation tests

Pure mineral flotation experiments and artificial mixed mineral flotation experiments are conducted according to standardized procedures. Initially, a precisely measured 2.000 g pure mineral sample was weighed using an electronic analytical balance. The weighed sample was transferred to a 40 mL flotation cell containing 36 mL deionized water. The slurry was agitated using an XFG-type mechanical agitation flotation machine operating at 1800 rpm. Sulfuric acid (0.1 M) or sodium hydroxide (0.1 M) solution was introduced to achieve the pre-determined pH range, followed by 3 min of stiring. Sodium fluorosilicate (100 mg·L^{-1}) was added as activator with 5 min agitation duration. Xanthate collector was introduced with subsequent 3 min mixing. The flotation process was maintained for exactly 3 min with manual froth skimming at 15 s intervals. Post-flotation processing involved oven-drying both concentrate and tailings products for 12 h until constant mass was achieved. Weigh the dried product and calculate the recovery rate. Repeat the test under the same conditions three times and take the average.

2.2.2. Batch flotation tests of real ore

Place 500g of mixed iron concentrate sample from Wanguo Gold Group Co., Ltd. in a 1.5L standard flotation cell. First, add pH regulator to adjust the slurry to a suitable pH level. Then, sequentially add SF, xanthate, and terpene oil as flotation reagents. The test process is a closed-circuit flotation process consisting of one roughing, one cleaning and one scavenging. The iron concentrate and sulfur concentrate products obtained during the flotation process are dried and weighed. The TFe and S contents are determined by titration, and the recovery rates of each component are calculated.

2.3. Analytical method

2.3.1. Contact angle measurements

Use sandpaper to polish block samples of three pure minerals of pyrrhotite and three pure minerals of magnetite until each mineral sample contains at least one relatively smooth surface. Block-shaped ore samples (pyrrhotite and magnetite) were encapsulated in silicone molds using an epoxy resin/hardener mixture (mass ratio of 2:1). The encapsulated samples were cured at 25°C for 6 hours. The mineral samples were polished using an automatic polishing machine. Pure water was added to the beakers of the first group of pyrrhotite samples and the first group of magnetite samples as raw ore samples; Add pure water and xanthate to the beakers of the second group of pyrrhotite samples and the second group of magnetite samples; Add pure water, SF, and xanthate to the beakers of the third group of pyrrhotite samples and the third group of magnetite samples. After standing for 60 minutes, the samples were removed with tweezers. The air-dried samples for 12 h were analyzed by the sessile drop method (DSA1005 contact angle meter, Kruss GmbH). Each sample was measured three times. Take the average of three measurements as the data for the bar chart.

2.3.2. FTIR measurements

Put three parts of pure mineral powder of pyrrhotite and three parts of pure mineral powder of magnetite used in the experiment into six beakers respectively. Add 40ml of pure water to all six beakers

and use an ultrasonic cleaning machine to shake for 5 minutes. After allowing to stand for another 5 minutes, discard the supernatant. Repeat the three operations of vibration, standing, and pouring the supernatant three times for six ore samples to achieve sample cleaning. Pure water was added to the beakers of the first group of pyrrhotite samples and the first group of magnetite samples as raw ore samples; Add pure water and xanthate to the beakers of the second group of pyrrhotite samples and the second group of magnetite samples; Add pure water, SF, and xanthate to the beakers of the third group of pyrrhotite samples and the third group of magnetite samples. Stir with a magnetic stirrer for 20 minutes. After standing for 3 minutes, discard the supernatant. Dry the remaining solid sample in an oven at 50 degrees Celsius.Fourier transform infrared spectroscopy analysis was conducted using a Spectrum Two spectrometer with a spectral resolution of 4 cm^{-1}. First, a background spectrum was obtained by scanning a pellet made from spectroscopic-grade KBr. The mineral powder (particle size less than 38 μm) was mixed uniformly with KBr at a mass ratio of 1:100. Pellets were then prepared using a stainless steel mold under the same pressing conditions. The transmission spectra were scanned in the range of 4000 - 400 cm^{-1}.

2.3.3. XPS measurements

X-ray photoelectron spectroscopy (XPS) analysis was performed using a PHI 5000 VersaProbe III system equipped with monochromatic Al-Kα radiation . The survey scans were conducted over the range of 1200 - 0 eV with a step size of 0.125 eV. The take-off angle of the sample stage was set to 45.0° relative to the surface normal. Energy calibration was achieved by referencing the C1s peak to a binding energy of 284.8 eV.

3. Results and discussion

3.1. Flotation separation behaviour of pyrrhotite and magnetite

3.1.1. Single-mineral flotation tests

Pyrrhotite, a chemically reactive sulfide mineral containing both Fe^{3+} and Fe^{2+} iron species, exhibits surface oxidation susceptibility (Qi et al., 2019; Rezvani et al., 2024). To enhance flotation efficiency and optimize process parameters, we systematically investigated the effects of pulp pH and xanthate dosage on the flotation behavior of pyrrhotite and magnetite under activated and non-activated conditions. In traditional craftsmanship, $CuSO_4$ is often used as an activator. Therefore, the influence of slurry pH value on the flotation behavior of pyrrhotite and magnetite under the conditions of $CuSO_4$ as activator and SF as activator was also studied. The variation of flotation recovery rate is shown in Fig. 3.

Under acidic conditions (pH 2-6), the surface reactions of pyrrhotite can be described by the following equations (Multani and Waters, 2018):

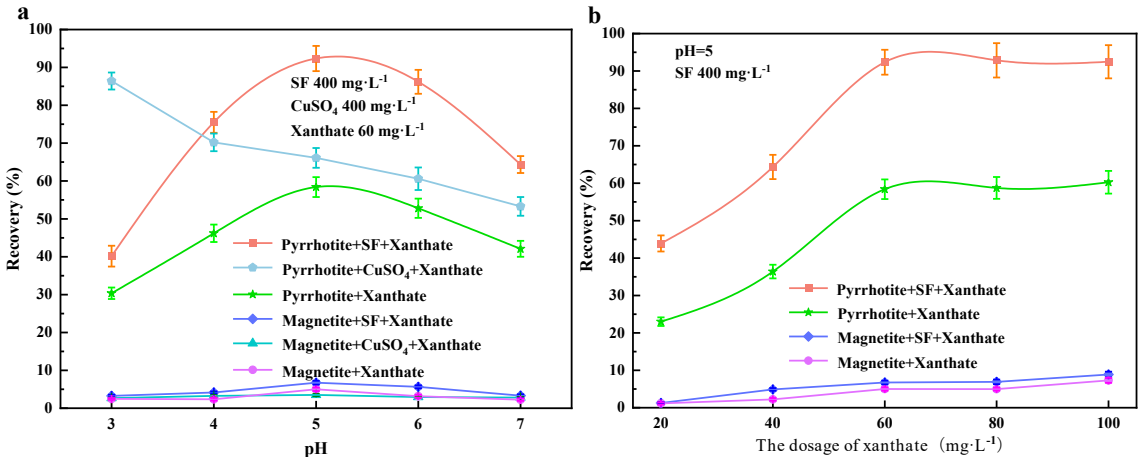

Fig. 3. Flotation recovery rates of pyrrhotite and magnetite as functions of pulp pH (a) and collector dosage (b)

$$Fe_{1-x}S + O_2 \rightarrow Fe^{2+} + {SO_2}^{2-} + H^+ \quad (1)$$

As evidenced by Fig. 3(a), magnetite exhibited flotation recoveries below 10% across all investigated reagent regimes, indicating its inherently poor floatability in this chemical system. In marked contrast, pyrrhotite demonstrated superior floatability under identical conditions. This differentiation arises from xanthate's selective chemisorption on pyrrhotite surfaces, where the collector forms stable hydrophobic complexes through specific chemical interactions with ferrous ions (Fe^{2+}). The predominant surface reaction can be described as (Tang and Chen, 2022):

$$Fe^{2+} + 2ROCSS^{-} \rightarrow Fe(ROCSS)_2 \quad (2)$$

The flotation recovery of pyrrhotite exhibited pH-dependent behavior in the presence of xanthate alone. As solution acidity decreased (pH 2-5), recovery increased progressively from 30.35% to 58.40%, correlating with reduced decomposition of xanthate. Under acidic conditions (pH <5), the thiolcarboxylate group (-CSS^{-}) in xanthate undergoes rapid decomposition to disulfides (CSSC) and carbon disulfide (CS_2), diminishing its collecting power (Elizondo-Álvarez et al., 2021; Wang et al., 2023). As the pH value increases, the decomposition rate of xanthate into disulfides or other products gradually decreases, leading to a corresponding increase in the effective concentration of xanthate . This enhances the flotation recovery rate of pyrrhotite, which peaks at 58.40 % when the pH is 5. However, further increasing the pH beyond this optimal point results in a gradual decrease in the flotation recovery rate. It is well established that $Fe(OH)_2$ begins to precipitate around pH 5. As the pH continues to increase, surface oxidation progressively intensifies, forming a hydrophilic layer that hinders the adsorption of collectors on the pyrrhotite surface. Consequently, the flotation recovery rate of pyrrhotite decreases as pH increases above 5.

The addition of activators significantly enhanced the flotation recovery rates of pyrrhotite under both experimental conditions. However, distinct optimal pH values were observed for the two activator systems. When CuSO4 was employed as the activator, the maximum flotation recovery of pyrrhotite was achieved at pH 3. In contrast, the use of SF as the activator resulted in peak recovery at pH 5. Notably, strongly acidic conditions are known to induce severe equipment corrosion in industrial applications. Therefore, SF has the best performance under weakly acidic conditions and is a more favorable choice of activator in actual mineral processing operations. The addition of SF significantly enhanced the flotation recovery of pyrrhotite (10-30% higher than the group without activator), demonstrating its pronounced activation effect on the mineral. This activation mechanism involves two synergistic pathways: (1) Fluoride ions (F^{-}) preferentially coordinate with Fe^{3+} in surface oxide layers to form soluble complexes (Lau et al., 2024), effectively removing passivating oxide coatings that hinder collector adsorption (Meng et al., 2023); (2) Subsequent exposure of fresh Fe-S surfaces increases available chemisorption sites for xanthate molecules, as evidenced by XPS analysis showing a increase in Fe^{2+} surface concentration. As shown in Fig. 3, the activation efficiency exhibited pH dependence, reaching maximum recovery (92.35 %) at pH 5. This correlates with the pH-dependent liberation of free F^{-} ions , which facilitates oxide dissolution through stable Fe^{3+}-F coordination. However, excessive alkalinity (pH > 6) induced surface re-oxidation. The generated iron oxide coating hinders the approach of collectors, reducing the recovery rate of pyrrhotite to below 65% when the pH is 7.

Fig. 3(b) systematically evaluated the dose-dependent flotation response of pyrrhotite and magnetite to xanthate with or without sodium fluorosilicate (SF) activation. Notably, magnetite exhibited poor floatability (recovery < 10% under test conditions), confirming the selectivity of the reagent system for pyrrhotite. Without sodium fluorosilicate, the flotation recovery of pyrrhotite gradually increased with increasing collector dosage. This trend indicates that an appropriate amount of collector can effectively promote the adhesion of pyrrhotite particles to bubbles, thereby enhancing recovery efficiency. The maximum recovery of 54.4% was achieved at a butyl xanthate dosage of 60 mg·L^{-1}, suggesting optimal interaction between the collector and pyrrhotite surface at this concentration. Further increases in collector dosage did not significantly improve recovery. However, in the presence of sodium fluorosilicate, the flotation recovery of pyrrhotite significantly increased. This result further validates the activation effect of sodium fluorosilicate on pyrrhotite flotation. Therefore, it can be concluded that sodium fluorosilicate has a significant activation effect on the flotation recovery of pyrrhotite, optimizing the flotation process and improving mineral resource utilization.

Based on the above results, it can be concluded that this flotation system demonstrates significant potential for effectively separating pyrrhotite from magnetite.

3.1.2. Flotation tests of mixed pure minerals

Single-mineral flotation tests revealed optimal separation efficiency between pyrrhotite and magnetite under the following conditions: pulp pH 5, sodium fluorosilicate dosage of 400 mg·L^{-1}, and butyl xanthate dosage of 60 mg·L^{-1}. A synthetic ore blend was prepared by combining pyrrhotite (S grade: 39.55%) and magnetite (S grade: 0.04%) at a 1:4 mass ratio, yielding a composite feed material with 7.74% sulfur content. Flotation separation experiments conducted under these optimized parameters (Fig.4) demonstrated distinct partitioning behavior: the concentrate exhibited a sulfur grade of 33.27% with 91.55% recovery, while tailings showed a significantly reduced sulfur grade of 0.83% and 8.45% recovery.

The pronounced sulfur enrichment in the concentrate (33.27% vs. feed grade 7.74%) confirms effective pyrrhotite upgradation. This selective recovery pattern indicates clear separation efficacy between pyrrhotite and magnetite under the specified reagent regime. The substantial sulfur grade differential (32.44%) between concentrate and tailings, coupled with complementary recovery distributions, provides robust evidence of successful mineral separation. These findings establish the proposed flotation conditions as a technically viable approach for pyrrhotite-magnetite separation systems.

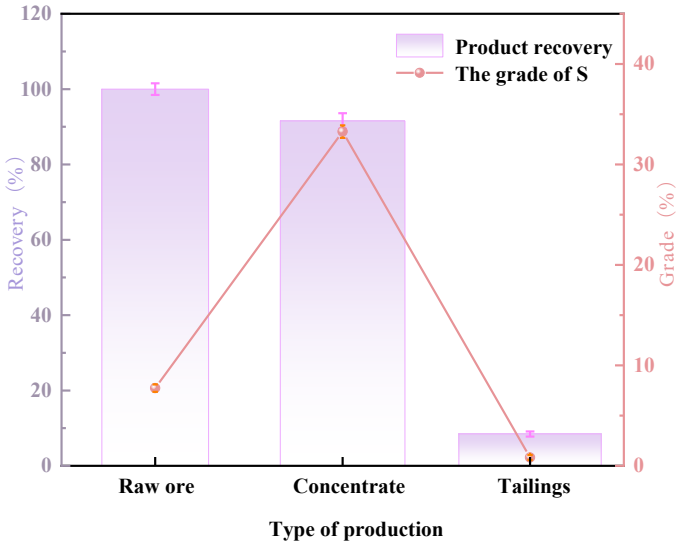

Fig. 4. Flotation test results of artificially mixed minerals

3.1.3. Flotation separation of pyrrhotite and magnetite from mixed iron concentrate

To systematically investigate the activation efficacy of SF in practical mineral processing, flotation tests were conducted on mixed iron concentrate samples from Wanguo Gold Group Co., Ltd. This study systematically investigates the flotation separation efficiency of pyrrhotite and magnetite in mixed iron concentrates under optimized conditions, employing sulfuric acid for pH regulation, SF as an activator, xanthate as the primary collector, and terpenic oil as the frothing agent. Based on the optimized parameters derived from conditional tests for pyrrhotite-magnetite separation, a closed-circuit flotation process comprising one roughing, one cleaning, and one scavenging stage was implemented. The detailed flotation process is illustrated in Fig. 5. In order to verify whether SF has a good activation effect in real ore flotation, a comparative experiment was conducted with and without SF as an activator. The experimental results are shown in Table 2.

According to Table 2, without adding SF as an activator, although the grade of S in sulfur concentrate increased to 4.67%, the grade of S in iron concentrate still remained at a high level of 2.13%. However, when SF was added as an activator, the grade of S in the sulfur concentrate increased to 9.15%, while the grade of S in the iron concentrate decreased to 0.32%. Notably, the sulfur content was significantly reduced from 2.60% to 0.32%, achieving a sulfur removal efficiency of 90.86%. Obviously, using SF as an activator effectively enhances the flotation separation effect of magnetite and magnetite, and achieves excellent mineral processing indicators. In addition, under the initial conditions of 61.34% iron content in the ore, the process ultimately obtained an iron concentrate with a yield of 75.20%, an iron

grade of 63.08%, and an iron recovery rate of 76.30%. This integrated approach confirms the dual benefits of SF-activated flotation technology - simultaneous sulfur impurity removal and iron grade enhancement, while maintaining industrially viable recovery rates.

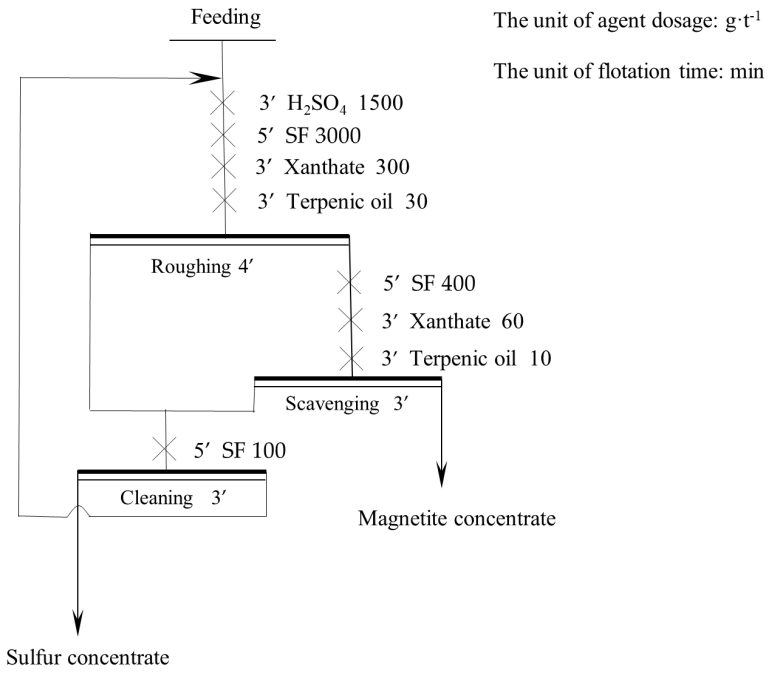

Fig. 5. Closed circuit tests flow of flotation separation of pyrrhotite and magnetite

Table 2. Chemical composition of pyrrhotite and magnetite (%)

Process	Product	Yield	Grade		Recovery	
			S	Fe	S	Fe
Without SF	Sulfur concentrate	18.43	4.67	58.53	33.13	17.58
	Magnetite concentrate	81.57	2.13	61.98	66.87	82.42
	Feeding	100.00	2.60	61.34	100.00	100.00
SF	Sulfur concentrate	25.80	9.15	56.35	90.86	23.70
	Magnetite concentrate	74.20	0.32	63.08	9.14	76.30
	Feeding	100.00	2.60	61.34	100.00	100.00

3.2. Flotation separation mechanism of pyrrhotite and magnetite

3.2.1 Contact angle analysis

In mineral processing systems, particularly in froth flotation operations, strategic application of flotation reagents modifies the physicochemical characteristics of mineral surfaces to achieve selective separation. The adsorption mechanism of collectors manifests through hydrophilic group anchoring to mineral surfaces and hydrophobic group orientation toward the aqueous phase, thereby enhancing surface hydrophobicity and bubble attachment capability. Contact angle measurements provide critical insights into liquid droplet spreading behavior on solid surfaces, serving as a quantitative indicator of surface hydrophobicity. Specifically, larger contact angles correlate strongly with enhanced hydrophobic characteristics and improved mineral floatability.

Systematic contact angle measurements were conducted on magnetite and pyrrhotite samples treated with various reagents, and the results are presented in Fig. 6. The experimental data reveal distinct response patterns: both reagents induced significant contact angle modifications in pyrrhotite ($\Delta\theta$ = +13.6° to +27.9°), while magnetite exhibited negligible changes. This selective surface response establishes a fundamental basis for differential flotation of iron-bearing minerals through reagent scheme optimization.

Notably, single xanthate treatment increased pyrrhotite's contact angle from 40.2° to 53.8° (34% enhancement), demonstrating effective hydrophobicity modification. The synergistic effect of sodium

fluorosilicate-xanthate combination further elevated contact angles to 68.1° - a 69% improvement over baseline values. These findings clearly demonstrate that the addition of sodium fluorosilicate exerts a distinct activation effect on pyrrhotite flotation, significantly enhancing the hydrophobicity of its surface.

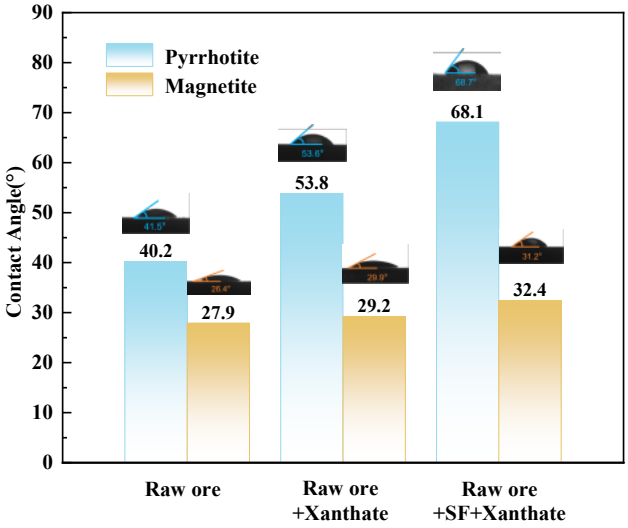

Fig. 6. Changes in the contact angle between pyrrhotite and magnetite before and after the action of the agent

3.2.2. FTIR analysis

Fourier transform infrared spectroscopy (FTIR) provides crucial molecular-level insights for optimizing flotation reagents and enhancing mineral surface modification by analyzing functional groups, adsorption behaviors, and interfacial reaction mechanisms. To investigate the adsorption mechanisms of sodium fluosilicate and xanthate on mineral surfaces, FTIR analyses were performed on pyrrhotite and magnetite samples before and after reagent treatment. The results are presented in Fig. 7.

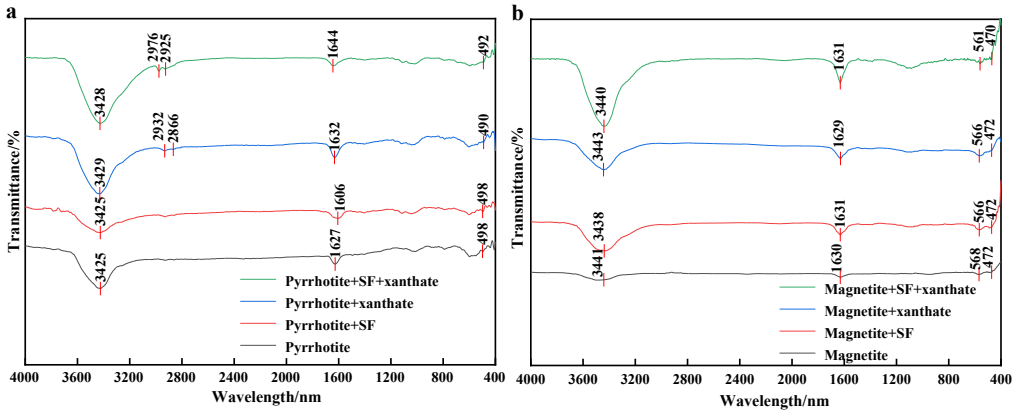

Fig. 7. FTIR spectra of magnetite (a) and magnetite (b) before and after agent action

Pyrrhotite, a chemically reactive sulfide mineral, exhibits pronounced surface oxidation susceptibility. As depicted in Fig. 7(a), distinct absorption bands persist at 498, 1627, and 3425 cm^{-1} in the FTIR spectra of pyrrhotite before and after reagent treatment. The Fe-O stretching vibration at 498 cm^{-1} (Mi et al., 2024), Fe-OH bending vibration at 1627 cm^{-1} (Yuan et al., 2022), and O-H stretching vibration at 3425 cm^{-1} (Yuan et al., 2022) collectively confirm hydroxylation and hydration states on the mineral surface. Sodium fluosilicate treatment induced a bathochromic shift of the Fe-OH bending vibration from 1627 to 1606 cm^{-1}, suggesting ligand substitution (e.g., F^- replacing -OH) and altered surface coordination. Xanthate adsorption was evidenced by emergent C-H stretching vibrations at 2866 and 2932 cm^{-1} (Zahoor et al., 2022), characteristic of alkyl chain interactions. Co-treatment with both reagents resulted in further spectral modifications: the Fe-OH band shifted to 1644 cm^{-1}, accompanied

by peak broadening and positional changes (2925/2976 cm^{-1}) in the C-H stretching region, indicative of synergistic adsorption and interfacial interactions between sodium fluosilicate and xanthate.

For magnetite (Fig. 7b), invariant absorption bands at 472, 568, 1630, and 3441 cm^{-1} were observed across treatments. The Fe-O vibrations at 568 cm^{-1} (tetrahedral sites) and 472 cm^{-1} (octahedral sites) (Della Ventura et al., 2022; Chubar et al., 2021), along with O-H stretching (3441 cm^{-1}) and H-O-H bending (1630 cm^{-1}) modes (Mi et al., 2024), reflect intrinsic structural features and surface hydration. The absence of spectral alterations post-treatment confirms negligible adsorption of sodium fluosilicate or xanthate on magnetite surfaces.

3.2.3 XPS analysis

To gain deeper insights into surface chemical modifications induced by reagent treatments, we conducted peak deconvolution analysis of F 1s and Fe 2p binding energy spectra for pyrrhotite surfaces under different treatment conditions, as shown in Fig. 8 and Fig. 9.

The strong electronegativity of F^- withdraws electron density from Fe^{3+}, consequently increasing the binding energy of Fe species. Notably, pristine pyrrhotite surfaces exhibited no detectable F 1s signals (Fig. 8). Following sodium fluosilicate treatment, a distinct F 1s peak emerged, deconvoluted into two components at 684.76 eV and 684.31 eV, both attributed to Fe^{3+}-F coordination complexes (Bahadur et al., 1993). These observations demonstrate the formation of stable Fe^{3+}-F surface complexes through chemisorption of fluorosilicate species.

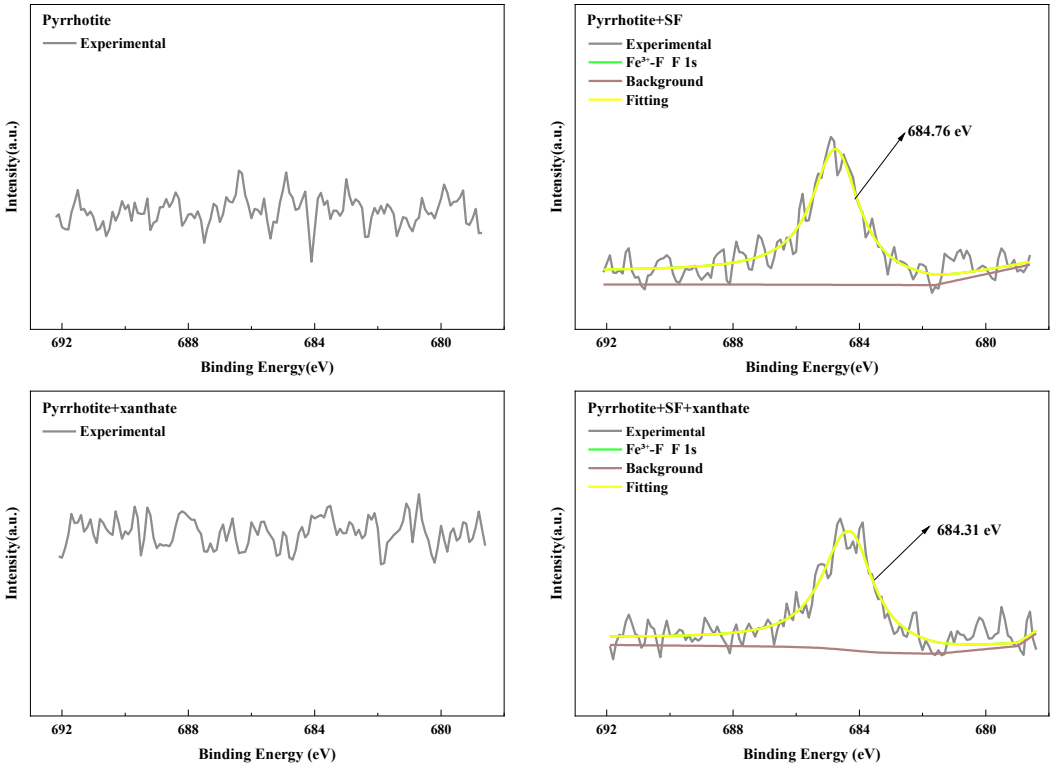

Fig. 8. High-resolution XPS spectra of F 1s on the surface of pyrrhotite before and after treatment

The Fe 2p XPS spectrum typically exhibits two primary spin-orbit split components, 2p3/2 and 2p1/2, with additional satellite peaks arising from multiplet splitting effects. The presence of different oxidation states (Fe^{2+} and Fe^{3+}) can lead to significant shifts in binding energy (BE). Pyrrhotite may contain multiple iron oxidation states, and the introduction of additives can alter its surface chemical environment. In a pure water system, the deconvolution of the Fe 2p spectra in Fig. 9 reveals the following assignments: 709.36 eV corresponds to the 2p3/2 main peak of Fe^{2+}-O, 710.59 eV to the 2p3/2 main peak of Fe^{3+}-OOH, 718.73 eV characterizes the tailing feature of the Fe^{3+} satellite peak, 722.58 eV is the 2p1/2 main peak of Fe^{2+}, 724.17 eV corresponds to the 2p1/2 main peak of Fe^{3+}, and 732.53 eV is attributed to the Fe^{3+} satellite peak (Wang et al., 2023; Zhang et al., 2018). The significantly higher peak intensity of Fe^{3+} compared to Fe^{2+} suggests the presence of a thick oxide layer on the surface.

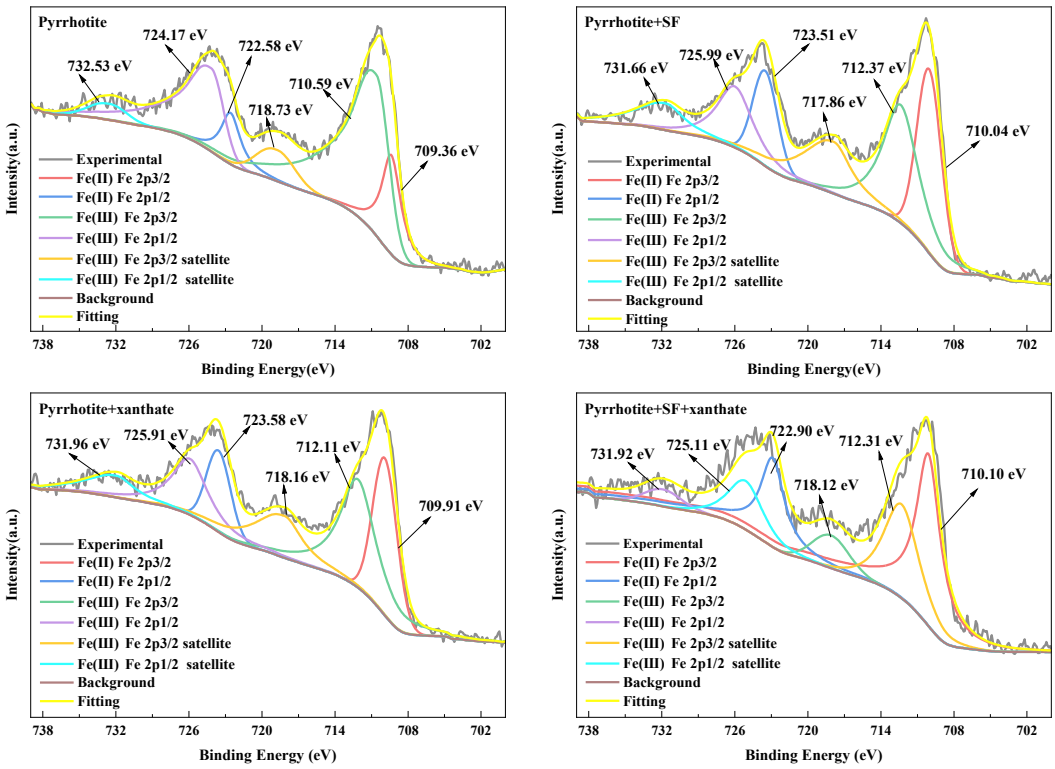

Fig. 9. High-resolution XPS spectra of Fe 2p on the surface of pyrrhotite before and after treatment

When sodium fluosilicate is added alone, the binding energies of the Fe^{2+} and Fe^{3+} main peaks exhibit pronounced positive shifts, while the binding energy of the Fe^{3+} satellite peak shows a pronounced negative shift. This indicates a significant alteration in the surface chemical environment of pyrrhotite. A new peak at 712.37 eV corresponds to the Fe^{3+}-F complex (Bahadur et al., 1993), indicating that sodium fluosilicate forms a stable Fe^{3+}-F complex on the mineral surface, consistent with the analysis results in Fig. 9. Additionally, the peak intensity of Fe^{3+} is significantly lower than that of Fe^{2+}, suggesting that the surface oxide layer has dissolved, exposing fresher Fe^{2+}-S surfaces on the pyrrhotite surface.

When xanthate is added alone, the binding energies of the Fe^{2+} and Fe^{3+} main peaks exhibit pronounced positive shifts, while the binding energy of the Fe^{3+} satellite peak shows a pronounced negative shift. The coordination of xanthate ($ROCSS^-$) pulls electrons towards the S atom, reducing the electron cloud density around Fe^{2+} and causing a positive shift in its binding energy. A new peak at 709.91 eV corresponds to $Fe(OCSS)_2$ (Szargan et al., 1992), indicating that xanthate undergoes chemical adsorption with Fe^{2+} on the surface of pyrrhotite, forming $Fe(ROCSS)_2$.

When sodium fluosilicate and xanthate are added simultaneously, the chemical environment of Fe undergoes significant changes. The binding energy of the Fe^{3+} main peak shifts to 712.31 eV, consistent with the Fe^{3+}-F complex peak. The binding energy of the Fe^{2+} main peak shifts to 710.10 eV, consistent with the $Fe(OCSS)_2$ peak. Compared to single-agent treatments, the peak area of Fe^{3+} decreases significantly, while the peak area of Fe^{2+} increases significantly. This suggests that prior treatment with sodium fluosilicate dissolves the oxide layer, exposing more Fe^{2+} active sites, thereby enhancing the availability of these sites for xanthate ($ROCSS^-$) adsorption.

3.2.4. Flotation separation mechanism

The xanthate system demonstrates superior floatability for pyrrhotite, primarily attributed to the chemisorption of xanthate anions ($ROCSS^-$) with surface Fe^{2+} species, forming $Fe(ROCSS)_2$ complexes. However, the presence of surface oxide layers significantly hinders xanthate adsorption on pyrrhotite. Pre-treatment with sodium fluosilicate (SF) effectively dissolves these oxide layers, thereby exposing additional Fe^{2+} active sites. This enhanced surface reactivity facilitates increased xanthate adsorption, leading to improved floatability of pyrrhotite. In contrast, neither SF nor xanthate exhibits detectable

adsorption on magnetite surfaces. This distinct adsorption behavior amplifies the floatability contrast between pyrrhotite and magnetite, enabling efficient flotation separation of the two minerals.

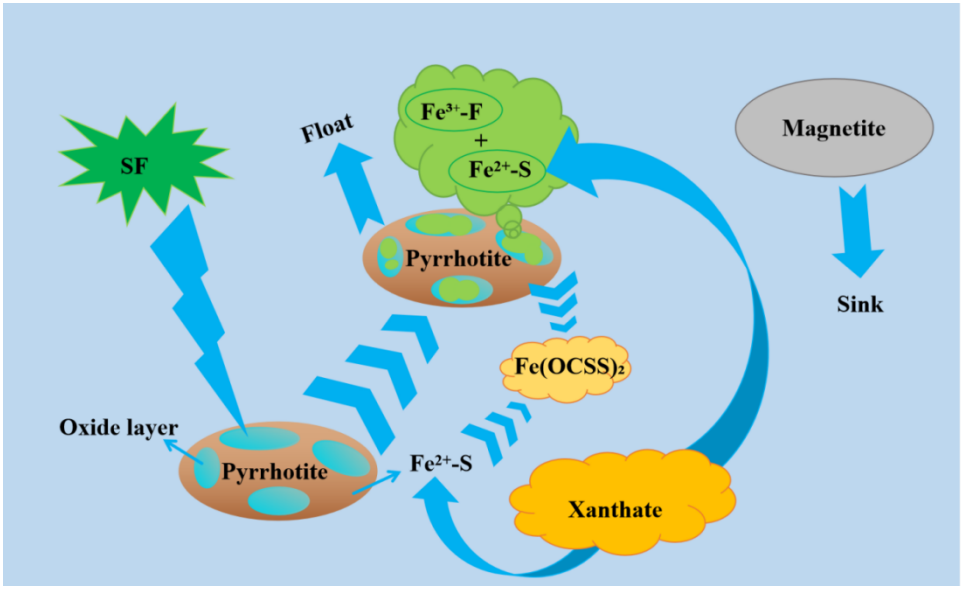

Fig. 10. Flotation model diagram of pyrrhotite and magnetite

4. Conclusions

Micro-flotation tests indicated that the activation effect of sodium fluosilicate on pyrrhotite flotation in the xanthate system was the strongest at pH 5. Under the conditions of pulp pH 5, sodium fluosilicate dosage of 400 mg·L^{-1} and butyl xanthate dosage of 60 mg·L^{-1}, artificial mineral flotation tests were conducted, obtaining a concentrate with S grade and recovery of 39.32% and 46.64% respectively, and a tailing with S grade and recovery of 2.72% and 53.36% respectively. Pyrrhotite and magnetite were efficiently separated by flotation.

For feed ore with an initial S grade of 2.60% and Fe grade of 61.34%, beneficiation yielded a sulfur concentrate with a mass yield of 25.80%, S grade of 9.15%, and S recovery of 90.86%, as well as an iron concentrate with a mass yield of 74.20%, Fe grade of 63.08%, and Fe recovery of 76.30%. This successfully achieved the dual objectives of iron enrichment and sulfur reduction.

Combined contact angle measurements, FTIR, and XPS analyses demonstrated selective adsorption of SF and xanthate exclusively on pyrrhotite surfaces. SF pretreatment effectively dissolved surface oxide layers, exposing additional Fe^{2+} active sites that facilitated enhanced xanthate anion ($ROCSS^-$) adsorption. This synergistic process significantly increased surface hydrophobicity, ultimately amplifying the floatability contrast between pyrrhotite and magnetite.

Acknowledgments

This research was supported by the Jiangxi Provincial Key Laboratory of Low-Carbon Processing and Utilization of Strategic Metal Mineral Resources (2023SSY01041).

References

ARVIDSON, B., KLEMETTI, M., KNUUTINEN, T., KUUSISTO, M., MAN, Y., HUGHES-NARBOROUGH, C., 2013. *Flotation of pyrrhotite to produce magnetite concentrates with a sulphur level below 0.05% w/w.* Miner. Eng. 50-51, 4-12.

ACAR, S., SOMASUNDARAN, P., 1992. *Effect of dissolved mineral species on the electrokinetic behavior of sulfides*. Miner. Eng. 5, 27-40.

BECKER, M., VILLIERS, J., BRADSHAW, D., 2010. *The flotation of magnetic and non-magnetic pyrrhotite from selected nickel ore deposits.* Miner. Eng. 23(11), 1045-1052.

BECKER, M., DE VILLIERS, J., BRADSHAW, D., 2010. *The mineralogy and crystallography of pyrrhotite from selected nickel and PGE ore deposits*. Econ. Geol. 105, 1025-1037.

BAHADUR, S., GONG, D., ANDEREGG, J., 1993. *Tribochemical studies by XPS analysis of transfer films of Nylon 11 and its composites containing copper compounds*. Wear 165, 205-212.

CHEN, Q., TIAN, M., ZHENG, H., LUO, H., LI, H., SONG, S., HE, D., JIANG, X., 2020. *Flotation of rutile from almandine using sodium fluorosilicate as the depressant*. Colloids Surf. A Physicochem. Eng. Asp. 599, 124918.

CHUBAR, N., GERDA, V., SZLACHTA, M., YABLOKOVA, G., 2021. *Effect of Fe oxidation state (+2 versus +3) in precursor on the structure of Fe oxides/carbonates-based composites examined by XPS, FTIR and EXAFS*. Solid State Sci. 121, 106752.

DAI, P., WEI, Z., CHEN, L., LIU, Y., 2022. *Adsorption of butyl xanthate on arsenopyrite (001) and Cu^{2+}-activated arsenopyrite (001) surfaces: a DFT study*. Chem. Phys. 562, 111668.

DONG, L., JIAO, F., QIN, W., ZHU, H., JIA, W., 2019. *Selective depressive effect of sodium fluorosilicate on calcite during scheelite flotation*. Miner. Eng. 131, 262-271.

DELLA VENTURA, G., RADICA, F., GALDENZI, F., SUSTA, U., CINQUE, G., CESTELLI-GUIDI, M., MIHAILOVA, B., MARCELLI, A., 2022. *Kinetics of dehydrogenation of riebeckite $Na_2Fe^{2+}_3Fe^{3+}_2Si_8O_{22}(OH)_2$: an HT-FTIR study*. Am. Mineral. 107, 754-764.

ELIZONDO-ÁLVAREZ, M., URIBE-SALAS, A., BELLO-TEODORO, S., 2021. *Chemical stability of xanthates, dithiophosphinates and hydroxamic acids in aqueous solutions and their environmental implications*. Ecotoxicol. Environ. Saf. 207, 111509.

HU, X., LUO, X., LIU, Z., ZHANG, Y., ZHOU, H., YANG, Z., TANG, X., 2024. *Flotation separation of feldspar from quartz using sodium fluosilicate as a selective depressant*. Rare Met. 43, 1288-1300.

LIAO, Y., ZHAO, G., FENG, B., YAN, H., WU, H., HU, W., ZHU, D., QIU, T., 2023. *Application of ultrasonic pre-treatment for flotation separation of pyrrhotite from chlorite*. Colloids Surf. A Physicochem. Eng. Asp. 669, 131507.

LIU, J., LI, E., JIANG, K., LI, Y., HAN, Y., 2018. *Effect of acidic activators on the flotation of oxidized pyrrhotite*. Miner. Eng. 120, 75-79.

LAU, K., ZEREBECKI, S., PIELSTICKER, L., HETABA, W., DHAKA, K., EXNER, K., REICHENBERGER, S., BARCIKOWSKI, S., 2024. *Fluoride substitution: quantifying surface hydroxyls of metal oxides with fluoride ions*. Adv. Mater. Interfaces 11, 2470064.

MULTANI, R., WATERS, K., 2018. *A review of the physicochemical properties and flotation of pyrrhotite superstructures (4C-Fe_7S_8/5C-Fe_9S_{10}) in Ni-Cu sulphide mineral processing*. Can. J. Chem. Eng. 96, 1185-1206.

Mikhlin, Yu., Kuklinskiy, A., Pavlenko, N., Varnek, V., Asanov, I., Okotrub, A., Selyutin, G., Solovyev, L., 2002. *Spectroscopic and XRD studies of the air degradation of acid-reacted pyrrhotites*. Geochim. Cosmochim. Acta. 66(23), 4057-4067.

MENG, Q., YUAN, Z., DU, Y., WANG, J., 2023. *Sulfuric acid pretreatment of oxidized pyrrhotite in flotation desulphurization of magnetite concentrate*. Miner. Eng. 203, 108347.

MI, N., YANG, M., WANG, X., SUN, Q., HE, J., DENG, S., FAN, T., 2024. *Cadmium sorption on γ-Al_2O_3 and goethite in the presence of silicate: insights from XRD and FTIR studies*. J. Soils Sediments 24, 2309-2317.

QI, C., KHALKHALI, M., GRUNDY, J., LIU, J., MALAINEY, J., LIU, Q., 2019. *Unraveling polymorphic pyrrhotite electrochemical oxidation by underlying electronic structures*. J. Phys. Chem. C 123, 26442-26449.

REZVANI, A., RAJI, F., FAN, R., KAPPES, R., PENG, Y., 2024. *Quantifying pyrrhotite superstructures in copper-gold ore flotation through synchrotron X-ray diffraction analysis*. Miner. Eng. 216, 108894.

REZVANI, A., RAJI, F., LIU, Q., Peng, Y., 2024. *Identification and quantification of pyrrhotite superstructures in base metal sulfide ore samples: A critical review.* Miner. Eng. 218: 108975.

REZVANI, A., RAJI, F., LIU, Q., Peng, Y., 2024. *Unveiling different pyrrhotite superstructures in copper-gold ore samples: Insights from advanced spectroscopic and microscopic characterization.* Miner. Eng. 206: 108536.

SZARGAN, R., KARTHE, S., SUONINEN, E., 1992. *XPS studies of xanthate adsorption on pyrite*. Appl. Surf. Sci. 55, 227-232.

TANG, X., CHEN, Y., 2022. *A Review of Flotation and Selective Separation of Pyrrhotite: A Perspective from Crystal Structures*. Int. J. Min. Sci. Technol. 32(4), 847-863.

WANG, X., CHEN, M., MA, L., LIU, P., ZHOU, J., SAPSFORD, D.J., 2023. *New strategy for sustainable treatment of residual xanthate in mineral processing wastewater by using natural pyrite*. Miner. Eng. 204, 108427.

WANG, J., REN, Y., WANG, P., 2023. *(Fe, F) co-doped nickel oxyhydroxide for highly efficient oxygen evolution reaction*. J. Mater. Chem. A 11, 4619-4626.

YU, J., GE, YY., CAI, XW., 2016. *The Desulfurization of Magnetite Ore by Flotation with a Mixture of Xanthate and Dixanthogen*. Minerals. 6(3): 70.

YUAN, Q., MEI, G., LIU, C., CHENG, Q., YANG, S., 2022. *A Novel Sulfur-Containing Ionic Liquid Collector for the Reverse Flotation Separation of Pyrrhotite from Magnetite*. Sep. Purif. Technol. 303, 122189.

YUAN, Q., MEI, G., LIU, C., CHENG, Q., YANG, S., 2022. *The utilization of BHA and SBX collector mixture for the flotation of moderately oxidized pyrrhotite*. Miner. Eng. 189, 107890.

ZAHOOR, N., KHAN, M.A.S., ASHRAF, G.A., JUNAID, M., GULBADAN, S., MAHMOOD, K.A., 2022. *Insight of terbium substitution on the structural, spectroscopic, and dielectric characteristics of the Ba–Mg–Fe–O system*. Ceram. Int. 49, 11563-11570.

ZHANG, P., HUANG, W., JI, Z., ZHOU, C., YUAN, S., 2018. *Mechanisms of hydroxyl radicals production from pyrite oxidation by hydrogen peroxide: surface versus aqueous reactions*. Geochim. Cosmochim. Acta. 238, 394-410.